



HAL
open science

Silver electrodeposition for multipactor mitigation

Julie Belfio, Mohamed Belhaj, Florica Lazar, Omar Jbara

► **To cite this version:**

Julie Belfio, Mohamed Belhaj, Florica Lazar, Omar Jbara. Silver electrodeposition for multipactor mitigation. International Workshop on Multipactor, Corona and Passive Intermodulation (MUL-COPIM 2022), Radio Frequency Equipment and Technology Section (TEC-EFE) of the European Space Agency; Technical University of Valencia, Oct 2022, Valence, Spain. hal-03931236

HAL Id: hal-03931236

<https://hal.science/hal-03931236v1>

Submitted on 9 Jan 2023

HAL is a multi-disciplinary open access archive for the deposit and dissemination of scientific research documents, whether they are published or not. The documents may come from teaching and research institutions in France or abroad, or from public or private research centers.

L'archive ouverte pluridisciplinaire **HAL**, est destinée au dépôt et à la diffusion de documents scientifiques de niveau recherche, publiés ou non, émanant des établissements d'enseignement et de recherche français ou étrangers, des laboratoires publics ou privés.

SILVER ELECTRODEPOSITION FOR MULTIPACTOR MITIGATION

Julie Belfio ⁽¹⁾⁽²⁾, Mohamed Belhaj ⁽¹⁾, Florica Lazar ⁽²⁾, Omar Jbara ⁽²⁾

⁽¹⁾ONERA,

Université de Toulouse F-31055 Toulouse, France

Email: Julie.belfio@onera.fr, mohamed.belhaj@onera.fr

⁽²⁾MATIM Laboratory

Université de Reims Champagne-Ardenne, Reims, France

Florica.lazar@univ-reims.fr; omar.jbar@uni-reims.fr

INTRODUCTION

The multipactor effect is an electron avalanche like phenomenon that can occur in microwave components under vacuum. This undesirable effect results from the synchronism between the Radiofrequency-wave and the electron emission phenomenon of microwave-components materials that may lead to an exponential increase of the electron density [1].

The new trend in the space telecommunication is to increase the RF power density that leads to an increased multipactor risk. To circumscribe this risk, an interesting strategy consists to produce rough surfaces at microscopic scale with low Total Electron Emission Yield (TEEY) [2]. For this purpose, many technics are used such as laser ablation [3], micro-porous by photolithography [4], copper nanowires [5] or micro-structured gold/silver coatings [6], etc. For monolithic components produced by 3D printing, a major part of these nowadays used solutions are difficult to apply or inapplicable. That why, in this work, we explore the capabilities of electrodeposition techniques to produce low TEEY surfaces. This technique (fluid) could be suitable 3D printed components in particular.

In this work, surface roughness was induced directly during the silver electrochemical deposition on nickel substrate at ambient temperature with a bath composition that responds to some green chemistry aspect as the suppression of toxic product as cyanide (REACH).

This paper was divided in two parts. In the first part, we describe the effect of bath compositions and electrodeposition parameters on the surface morphology. In the second part, we present the effect of these surfaces on the TEEY. We will show that some produced morphologies lead to a substantial overall decrease of the TEEY. A scanning electron microscopy with electron dispersive X-Ray analysis were used to link the TEEY to surface morphology and chemical composition.

MATERIALS AND METHODS

1- Electrodeposition method

Silver coatings have been deposited on a nickel substrate by chronopotentiometry at ambient temperature. Five bath compositions, inspired by Zarkadas et al. [7] and Papanastasiou [8] (Table 1) were used to deposit silver on nickel.

Table 1. Bath composition and electrodeposition parameters to realize silver coatings

Name of samples	AgNO ₃ mol/L	HNO ₃ mol/L	Citric ac. mmol/L	Tartaric ac. mmol/L	Current density j _p (mA/cm ²)	Pulse on time (t _{on}) (min)	Total time deposition (min)
100C	0.2	0.1	15	0	-1	2	30
75C/25T			11.25	3.75			
50C/50T			7.5	7.5			
25C/75T			3.75	11.25			
100T			0	15			

Before the deposition, nickel substrate is pickled in HCl at 37 %w/w for 60s followed by rinsing with distilled water. Then, the dispositive for the deposition was a three electrodes cell (Fig. 1) with:

- Ag/AgCl bridge as a reference electrode (RE),
- A platinum plate with a surface of 1 cm² as a counter electrode (CE),
- Nickel plate with a surface of 25x25 mm² as a working electrode (WE) (Fig. 2).

These electrodes were connected to a potentiostat-galvanostat PGZ 100 Radiometer Analytical controlled by VoltaMaster 4 software. Finally, to obtain silver coatings with a good adherence, pulse galvanostatic method was chosen for a duration of 30 min with pulse (t_{on}) of 2 min and (t_{off}) of 10 s as shown in Fig. 3.

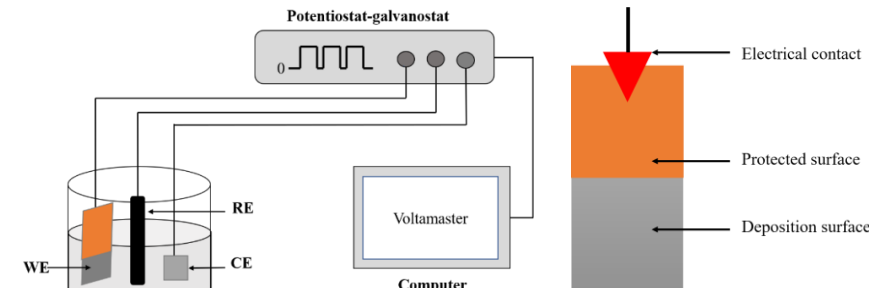


Fig. 1. Experimental set up

Fig. 2. Nickel plate for electrodeposition (WE)

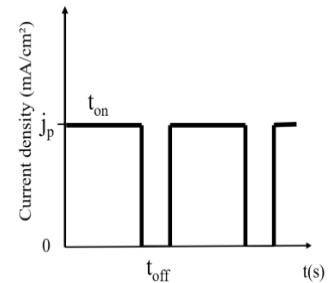


Fig. 3. Explanation of the pulse mode

2- Characterization

The morphology and the chemical composition of the deposits were investigated using a JEOL 6460 LV Scanning Electron Microscope (SEM) working at an accelerating voltage of 20 kV and coupled to an energy dispersive spectroscopy (EDS) detector (acquisition time 300 s). A semi-quantitative analysis is carried out by averaging measurements taken in three different places of the samples but of the same surface (magnification of 500).

Crystalline structure of the samples was studied by X-ray diffraction (XRD) using Bruker D8 Advance diffractometer with $\text{CuK}\alpha$ radiation ($\lambda_{\text{CuK}\alpha} = 1.5418 \text{ \AA}$), operating in Bragg-Brentano geometry, for 2θ ranging from 20° to 90° , with a step of 0.04° and a scan speed of 5 s by step. The crystallographic phases were analyzed using the JCPDS data basis with EVA 4 software. All the diagrams were set from the lines of substrate and normalized with respect to the most intense Ag peak. In all patterns, the peaks denoted by an asterisk are those relative to the substrate (Ni: 00-004-0850).

The roughness of the Ag coatings was measured using an optic profilometer using OLS LEXT31000 on an area of $49.9 \times 10^3 \mu\text{m}^2$. Different types of roughness were extracted:

- R_a : Arithmetic mean roughness of the profile. This allows the global evaluation of the amplitude of the profile roughness.
- R_c : This represents the average height of the profile elements.
- R_{zjjs} : This represents the ten-point arithmetic average of the five highest peaks and the five deepest valleys of the profile.

For all the characterization methods, the analyses were carried out on the same surface at the center of the deposit in order to avoid edge effects.

3- TEEY measurement

The measurements of the TEEY were performed in DEESSE facility [34] in a vacuum level of about 10^{-9} mbar and at room temperature of 23°C . An EGL-1022 Kimball electron gun with electron beam pulsing capabilities was used as the electron source. A schematic layout of the experimental setup is shown in Fig. 4. The sample was negatively biased to -9V during TEEY to avoid low energy secondary electrons and tertiary electrons to be recollected or collected by the sample.

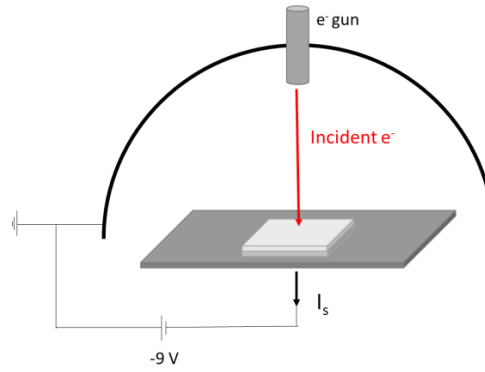


Fig. 4. Schematic diagram of the TEEY measurement setup

In the present, experiments incident electron pulses of 6 ms duration and few tens of nA current were used to avoid the electron beam induced conditioning effect. For each sample, the TEEY measurement was repeated 10 times. The derived standard deviation is typically lower than 2%. For all the incident electron energies of interest, the incident charge per pulse, ΔQ_i and the sample charge ΔQ_s per pulse were measured. The TEEY can be deduced from the following expression:

$$\text{TEEY} = \frac{\Delta Q_i - \Delta Q_{is}}{\Delta Q_i}$$

A full description of the measurement method can be found in the reference [35]. TEEY value of silver coatings deposited by electrodeposition has been compared with the TEEY performance of rolled silver reference plate (99.95 % purity, provide by Goodfellow).

RESULTS AND DISCUSSION

1- Influence of the electrochemical parameters on the deposit

After the deposition, all the samples were analysed by SEM, XRD and profilometry to notice the influence of the bath composition on the surface morphology.

Firstly, Fig. 5 shows the influence of the bath composition on the particle's morphology. Bath with only tartaric acid (100T) produce cubic particles in comparison with bath containing citric that produce acicular particles. These results show that during the deposition the reaction mechanism with citric acid is priority compared to the one with tartaric acid.

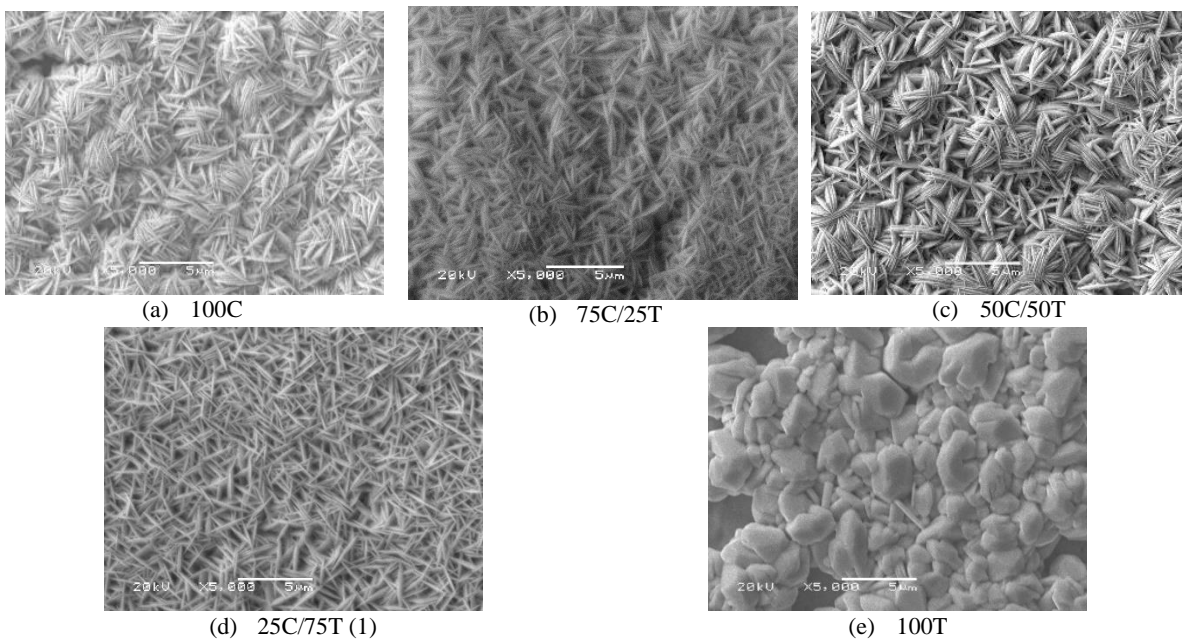


Fig. 5. SEM representation of silver coatings with 100C, 75C/25T, 50C/50T, 25C/75T and 100T baths

Secondly, samples were analysed by XRD to confirm the composition of these coatings (Fig. 6) and to obtain information concerning the crystallographic phases. The results confirm the silver coating formation on nickel substrate. Moreover,

this analysis gives a first explanation for the difference of the silver particle's shapes. In fact, silver coatings deposited using a citric acid based bath are a mixture of cubic phase (Ag 3C) and hexagonal phase (Ag 4H). In addition, silver coatings deposited in tartaric acid bath (100T) are formed only constitute cubic phase (Ag 3C). This result gives us an important information on the silver electrodeposition mechanism in comparison with the literature [7–9]. It will be interesting to deeper this in a future work.

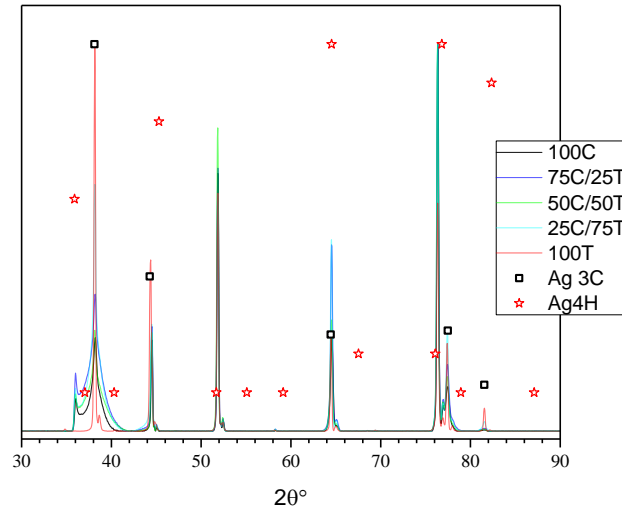


Fig. 6. XRD results for silver coatings deposited in 100C, 75C/25T, 50C/50T, 25C/75T and 100T baths

Profilometry was also used to have some information on the roughness. The three parameters (R_a , R_c and R_{zjis}) are derived (see Table 2). Qualitative analyses of the surface homogeneity were also done. The effect of the bath composition on the surface morphology is obvious.

Sample 100T presents a high difference between the other samples; this is explained by two facts: the difference of shapes particles and the difference of homogeneity. This lack of homogeneity is present in the Fig. 7 with a comparison with 25C/75T and 100T baths

Table 2. Roughness values for silver coatings electrodeposited in 100C, 75C/25T, 50C/50T, 25C/75T and 100T baths

	100C	75C/25T	50C/50T	25C/75T (1)	100T
R_a (μm)	0.551	0.545	0.633	0.491	1.048
R_c (μm)	1.18	1.008	1.234	1.196	2.211
R_{zjis} (μm)	10.158	11.41	11.298	10.403	14.04

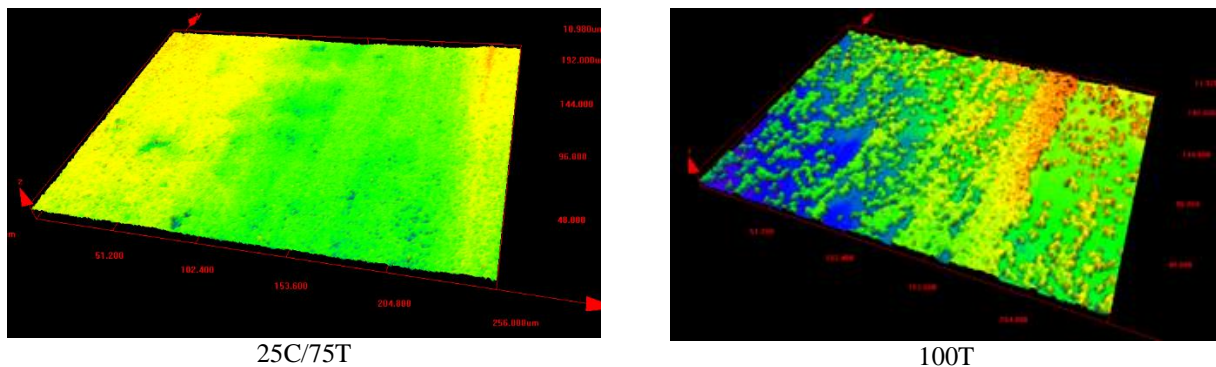


Fig. 7. 3D representations for silver coatings electrodeposited in 25C/75T and 100T baths

2- Influence of the surface morphology on the TEEY

The next step is to study the difference of surfaces morphology and to link these results to the electronic emission. All samples were analysed by DEESSE facility and were compared to a standard silver plate. Results are presented in the Fig. 8. This analyse show that all the silver coatings obtained by electrodeposition give best result than the standard for $TEEY_{max}$ (the maximum of the TEEY) and E_{C1} (the first crossover energy at which the TEEY is t equal to one). Two

samples have particularly low TEEY: 75C/25T and the 25C/75T with respectively: $E_{C1} = 45$ eV, $TEEY_{max} = 1.6$, and $E_{C1} = 46$ eV, $TEEY_{max} = 1.62$; in comparison with standard Ag: $E_{C1} = 27.4$ eV, $TEEY_{max} = 2.23$. The less interesting results is for the 100T sample. Different fact can explain this difference, the first fact is the different of shape for silver particles and the second fact is a bad homogeneity for the coating.

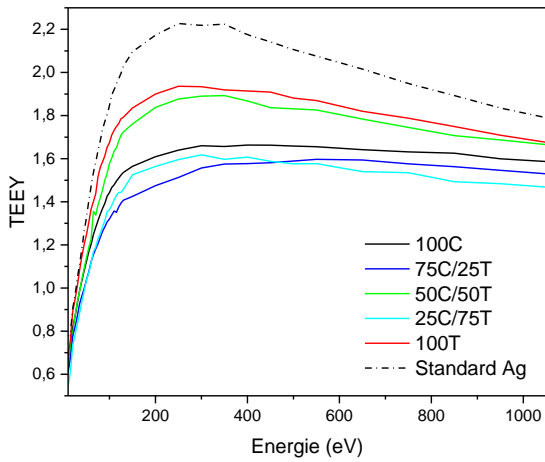


Fig. 8. TEEY representation for silver standard and for silver coatings electrodeposited in 100C, 75C/25T, 50C/50T, 25C/75T and 100T baths

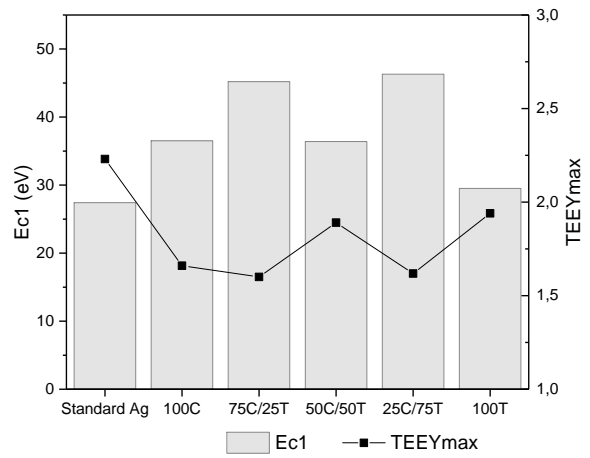


Fig. 9. $TEEY_{max}$ and E_{C1} trend for silver standard and for silver coatings electrodeposited in 100C, 75C/25T, 50C/50T, 25C/75T and 100T baths

An interesting point in regard to multipactor mitigation [10], the decrease of the $TEEY_{max}$ is coupled with the increase of E_{C1} (see Fig. 9)

Different studies show the influence of the roughness on the TEEY [11,12]. Fig. 10 shows the ratio Ra/Rc and E_{C1} evolution for all the baths. A net correlation between Ra/Rc ratio and E_{C1} was observed. Higher is this ratio and higher is E_{C1} .

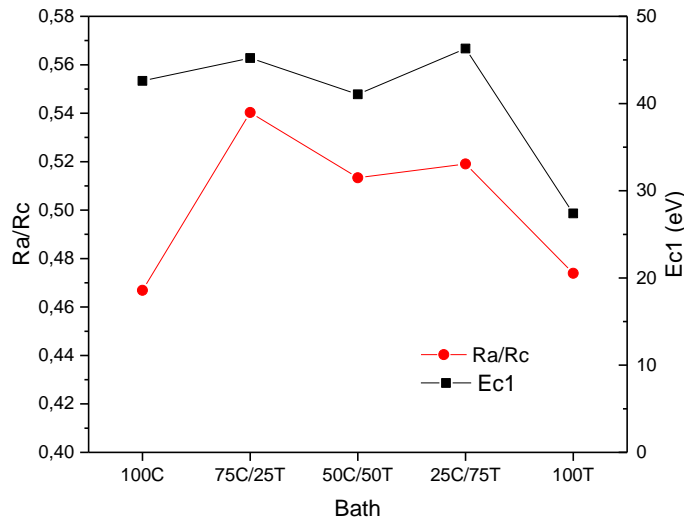


Fig. 10. Ratio Ra/Rc compared to E_{C1} for silver coatings with 100C, 75C/25T, 50C/50T, 25C/75T and 100T baths

In conclusion, to decrease the TEEY, we should favour bath with citric and tartaric acid, which induce silver particles with acicular shape. This particle shape is particularly good to act like an electron trap to decrease the $TEEY_{max}$ and increase the E_{C1} .

A reproducibility of the whole electrodeposition process to TEEY measurement has been realized for the silver coating 25C/75T. Six samples were realized in the same conditions, in the 25C/75T baths prepared six times by two distinct operators. Fig. 11 represents the average of TEEY. The standard deviation (2σ) envelope is also shown. The reproducibility of the process is quite good. The reproducibility of this TEEY reduction method is quite good but can still

be improved. In any case, even considering the higher TEEY, the silver deposition method presented here is still very interesting compared to conventional silver plating shown in the same graph.

The small observed disparity is probably due to a small variation of particles sizes, some heterogeneity of the coatings and some variation on the surface contamination after exposure, days and weeks to ambient atmosphere [13].

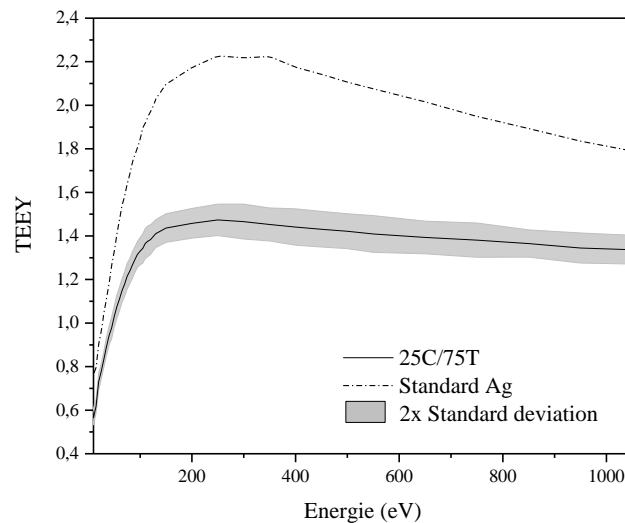


Fig. 11. Reproducibility of the TEEY measurement with 25C/75T bath

This study of reproducibility present that silver deposition method presented a very interesting compared to standard silver sample, even considering the higher TEEY.

CONCLUSION

This work focused on the development of silver anti-multipactor coatings based on tuning the surface roughness. The electroplating technique has been used to create an appropriate micrometric or submicron surface roughness in order to substantially improve the characteristics of the standard silver commonly used for high power RF devices. The deposition technic and methodology (bath composition, electrodeposition parameters) presented here allowed a significant overall lowering of the TEEY. The surface morphology and composition analyses permitted to link the TEEY drop to quantitative morphologic parameters. This opens a new perspective to further optimize the surface morphology (and thus the TEEY) through the tuning of the electrodeposition parameters.

Compared to the techniques currently used for multipactor mitigation for space applications, the proposed method will have few advantages:

- it can be applied in principle to complex geometry including monolithic microwave devices,
- it can be implanted at low cost in standard manufacturing process,
- it is fully compliant with the European Registration, Evaluation and Authorisation of Chemicals (REACH).

REFERENCES

- [1] M.A. Furman, *Electron Cloud Effects in Accelerators*, (2013).
- [2] J. Pierron, C. Inguibert, M. Belhaj, J. Puech, M. Raine, "Effect of rectangular grooves and checkerboard patterns on the electron emission yield", *Journal of Applied Physics*. 124 (2018) 095101.
- [3] R. Valizadeh, O.B. Malyshev, S. Wang, T. Sian, M.D. Cropper, N. Sykes, "Reduction of secondary electron yield for E-cloud mitigation by laser ablation surface engineering", *Applied Surface Science*. 404 (2017) 370–379.
- [4] M.(叶 鸣) Ye, Y.N.(贺永宁) He, S.G.(胡少光) Hu, R.(王瑞) Wang, T.C.(胡天存) Hu, J.(杨晶) Yang, W.Z.(崔万照) Cui, "Suppression of secondary electron yield by micro-porous array structure", *Journal of Applied Physics*. 113 (2013) 074904.
- [5] L. Aguilera, I. Montero, M.E. Dávila, A. Ruiz, L. Galán, V. Nistor, D. Raboso, J. Palomares, F. Soria, "CuO nanowires for inhibiting secondary electron emission", *J. Phys. D: Appl. Phys.* 46 (2013) 165104.
- [6] V. Nistor, L. Gonzalez, L. Aguilera, I. Montero, L. Galán, U. Wochner, D. Raboso, "Multipactor suppression by micro-structured gold/silver coatings for space applications", *Applied Surface Science*. (2014).

- [7] G.M. Zarkadas, A. Stergiou, G. Papanastasiou, "Influence of citric acid on the silver electrodeposition from aqueous AgNO₃ solutions", *Electrochimica Acta*. 50 (2005) 5022–5031
- [8] G. Papanastasiou, D. Jannakoudakis, J. Amblard, M. Froment, "Influence of tartaric acid on the electrodeposition of silver from aqueous AgNO₃ solutions", *Journal of Applied electrochemistry* (n.d.) 6.
- [9] J. Vereecken, R. Winand, "Influence of Inhibitors on the Structure of Silver Deposits Obtained by Electrolysis of Aqueous Nitrate Solutions", *Journal electrochem. Soc.* (1976) 4.
- [10] N. Fil, M. Belhaj, J. Hillairet, J. Puech, "Multipactor threshold sensitivity to total electron emission yield in small gap waveguide structure and TEEY models accuracy", *Physics of Plasmas*. 23 (2016) 123118.
- [11] J. Pierron, "Modèle de transport d'électrons à basse énergie (~10 eV- 2 keV) pour applications spatiales (OSMOSEE, GEANT4)", These de doctorat, Toulouse, ISAE, 2017.
- [12] C. Jin, A. Ottaviano, Y. Raitses, "Secondary electron emission yield from high aspect ratio carbon velvet surfaces", *Journal of Applied Physics*. 122 (2017) 173301.
- [13] T. Gineste, M. Belhaj, G. Teyssedre, J. Puech, "Investigation of the electron emission properties of silver: From exposed to ambient atmosphere Ag surface to ion-cleaned Ag surface", *Applied Surface Science*. 359 (2015) 398–404.